npj | climate and atmospheric science

www.nature.com/npjclimatsci

ARTICLE OPEN

Check for updates

Urban irrigation reduces moist heat stress in Beijing, China

Shuai Sun[1,2,3], Qiang Zhang[4]✉, Chunxiang Shi[1], Vijay P. Singh[5,6], Tao Zhang[1], Junxia Gu[1], Gang Wang[2], Wenhuan Wu[7], Donghui Chen[1] and Jianmei Wu[8]

Although urban irrigation can modulate local hydrothermal conditions and mitigate urban heat island effects, its impact on moist heat stress (MHS) is poorly understood. Employing the Weather Research and Forecasting Single-Layer Urban Canopy Model (WRF-SLUCM), we evaluated the effect of urban irrigation on the MHS in Beijing, China, and found that the updated initial soil moisture (SM) field improved the simulation of temperature, relative humidity, and wind speed. Besides, urban irrigation reduced urban and rural MHS, and particularly reduced afternoon and evening MHS by up to 1.2 °C but increased morning MHS by up to 0.4 °C. In addition, the effect of different irrigation times on MHS showed that irrigation at 02 and 20 h increased urban and rural MHS, with the best cooling effect at 00 and 13 h, which reduced the MHS by up to 2.65 °C in urban areas and 0.71 °C in rural areas. The findings highlighted mechanistically the effect of urban irrigation on MHS and shed light on how to mitigate urban heat island effects on urban sustainable development.

npj Climate and Atmospheric Science (2024)7:36 ; https://doi.org/10.1038/s41612-024-00585-6

INTRODUCTION

The global climate changes and rapid urbanization have resulted in intense urban heat islands and exacerbated heat stress in cities around the world, posing threats to human health[1,2]. Beijing, as the capital and the national central city of China, has experienced rapid urbanization. Beijing's urban areas are typical "heat islands", with heat island intensity significantly higher than that of China's coastal cities, resulting in lengthened summer heat periods, which seriously affect agricultural and industrial production, as well as the life and health of urban residents[3,4]. Therefore, urban heatwaves have aroused considerable concern in recent years[5,6].

To address growing urban heat island effects, strategies have been proposed to alleviate them, such as urban greening, green and cool roofs/walls, solar photovoltaic panels, urban irrigation, etc. Particularly, urban irrigation is an emerging, green, and sustainable strategy for reducing urban temperatures. Jeong et al.[7] indicated that urban irrigation could alleviate high temperatures while increasing relative humidity and removing some of the thermal comfort benefits in the Kansas City Metropolitan Area. Yuan et al.[8] showed that irrigation or artificial rainfall can mitigate surface urban heat island intensity (SUHI) in low-rainfall areas over the globe. Davis et al.[9] found decreased hot nights in the Indo-Gangetic Plain during 1951–2016 and reduced SUHI in major urban areas in India due to intensive irrigation. Gao et al.[10] found the cooling effects of additional irrigation in New South Wales and observed close relations between the cooling effects of additional irrigation and ambient temperature, urban fraction, as well as soil moisture before irrigation. Wang et al.[6] indicated that urban irrigation effectively mitigated heat stress, and its cooling effects improved human thermal comfort at night, while the increased humidity outweighed the cooling effect and exacerbated human thermal discomfort during daytime in Nanjing, China.

A multitude of studies have shown that relative humidity is a critical driver behind heatwaves and is directly related to human-heat exchange, human thermal comfort, and heat-related mortality and morbidity[11,12]. Relative humidity can amplify the magnitude and peak temperature of heat waves[11,13]. Besides, thermo-biological evidence necessitates relative humidity and wind speed in the evaluation of the impacts of heatwaves on human health[14]. Therefore, we introduced relative humidity and wind speed into the analysis of urban heatwaves.

In addition, the method, timing, and volume of irrigation are heavily controlled by human activities and hence have variable effects on local air temperature, surface temperature, relative humidity, and evapotranspiration. Guo et al.[15] found that the expansion of irrigated cropland exacerbated urban moist heat stress in northern India. Liu et al.[16] studied the effects of urban irrigation water on temperature in Beijing and found that the most effective way to reduce urban temperature by about 1.9 °C is to use 90% of the total urban water supply in Beijing for urban irrigation and 10% for road sprinkling. However, how does the timing of irrigation impact MHS? This question has not been well answered, especially for such a world's first-tier city as Beijing.

Current studies on urban heat-related research in Beijing have mainly focused on the spatial and temporal evolution of Beijing's summer heat and its mechanism[17,18], urban land use changes[19,20], anthropogenic heat[21,22], and the impact of urban heat island on precipitation and pollutants[23–25], while few studies paid attention to the effect of irrigation on urban heat in Beijing. Therefore, we took Beijing as a case study area and used WRF-SLUCM to explore (1) how to improve the simulation accuracy of MHS, (2) the effect of urban irrigation on urban and rural MHS, and (3) the effect of irrigation on MHS at different irrigated-time periods. This study can act as a reference for better mitigation of urban MHS, urban human health, and urban sustainable development.

RESULTS

Validation of WRF-SLUCM simulation

To better reflect the MHS in Beijing, we used the National Centers for Environmental Protection Final dataset (FNL), the first-generation Chinese atmospheric reanalysis (CRA), and the

[1]National Meteorological Information Center, China Meteorological Administration, Beijing, China. [2]Faculty of Geographical Science, Beijing Normal University, Beijing, China. [3]Key Laboratory of Coupling Process and Effect of Natural Resources Elements, Beijing, China. [4]Advanced Interdisciplinary Institute of Environment and Ecology, Beijing Normal University, Zhuhai, China. [5]Department of Biological and Agricultural Engineering, Zachry Department of Civil and Environmental Engineering, Texas A&M University, College Station, TX, USA. [6]National Water and Energy Center, UAE University, Al Ain, UAE. [7]Beijing Research Institute of Uranium Geology, Beijing, China. [8]Zhucheng Meteorological Administration, Shandong Province, Zhucheng, China. ✉email: zhangq68@bnu.edu.cn

updated initial soil moisture in CRA using high-quality China Meteorological Administration Land Data Assimilation System datasets (CRA_CLDAS) to drive the WRF-SLUCM for the simulation of temperature, relative humidity, and wind speed in Beijing, and validated the simulation results using the observation data. It can be found from Supplementary Fig. 2 and Supplementary Table 2 that CRA_CLDAS temperature, relative humidity, and wind speed in Beijing were better than CRA and FNL, so we chose CRA_CLDAS to drive the WRF-SLUCM for the simulation of urban irrigation on MHS. One interesting point is that updating the initial condition of soil moisture reduced the bias of temperature by 41.36% for urban areas and 58.52% for rural areas from a comparison of CRA_CLDAS and CRA, and both relative humidity and wind speed also improved. Improving the initial soil moisture condition can improve the model simulation. Soil moisture is critical in the heat and water vapor exchange between the lower boundary and the atmosphere, and improved soil moisture simulation can enhance numerical weather simulation[26,27].

Effect of urban irrigation on land surface variables

The WRF-SLUCM was driven by CRA_CLDAS separately to obtain air temperature, relative humidity, wind speed, sensible heat flux, latent heat flux, soil heat flux, land surface temperature, soil moisture, and planetary boundary layer in Beijing under irrigated and non-irrigated conditions, and the differences between them were calculated (Section 2.2 of Supplementary Information). It can be found that urban irrigation in Beijing reduced air temperature, soil heat flux, land surface temperature, and planetary boundary layer height in the urban and rural areas, reduced wind speed in urban areas and surrounding areas, and increased soil moisture in urban areas and relative humidity in urban and rural areas.

In addition, further verifying the impacts of irrigation on the urban heat island effect requires the calculation of the urban heat island index (denoted as T2_UHI LST_UHI, respectively) under irrigation and non-irrigation conditions using air and surface temperatures. We found that irrigation reduces the urban heat island in general (Section 2.3 of Supplementary Information).

Impact of urban irrigation on MHS

To further analyze the effect of urban irrigation on humid heat, the differences between the three indices of the Humidex (HI), the Apparent Temperature (AT), and the Steadman Index (SI) were calculated for irrigated and non-irrigated conditions during daytime (00:00–10:00, 23:00 UTC) and nighttime (11:00–22:00 UTC), respectively. It can be found that urban irrigation reduced the AT and SI indices in urban areas while the HI index increased (see Supplementary Fig. 5 in Supplementary Information).

To further quantify the effects of urban irrigation on MHS in urban and rural areas, we analyzed the daily variations of air temperature, relative humidity, and wind speed and calculated three humid-heat indices, respectively. In terms of temperature (Fig. 1a), urban irrigation can better reduce the temperature in urban areas than in rural areas, where the temperature in urban areas can be reduced by a maximum of 3 °C, especially just after irrigation (after 13 UTC), the temperature in rural areas can be reduced by a maximum of 0.5 °C. This finding is in good line with those by Liu et al.[16] that water sprinkling, including urban sprinkling and road sprinkling, reduced the overall Beijing temperature by 1.9 °C and that urban sprinkling changed latent and sensible heat fluxes and was able to reduce more than 3 °C for the city[28,29]. In terms of relative humidity (Fig. 1b), urban irrigation can increase the relative humidity of urban areas in a larger magnitude than rural areas, where relative humidity in urban areas increased by up to 26%, especially just after irrigation (after 13UTC), and relative humidity in rural areas increased by up to 5%. In terms of wind speed (Fig. 1c), urban irrigation reduced urban wind speed, especially just after irrigation, while urban irrigation had little effect on wind speed in suburban areas. It can be seen from the AT index (Fig. 1d) that urban irrigation had a greater effect on AT in urban areas than in rural areas, in which urban irrigation reduced AT in the afternoon and evening, with a maximum reduction of 1.2 °C, but urban irrigation increased AT up to 0.4 °C in the morning. Urban irrigation also had a cooling effect on AT in suburban areas, with a maximum reduction of 0.6 °C, mainly in the afternoon and evening periods. From the HI index (Fig. 1e), the cooling effect of urban irrigation was mainly in the afternoon and evening, with a maximum reduction of 1.2 °C in urban areas and a maximum reduction of 0.7 °C in rural areas, but urban irrigation increased MHS in urban areas at daytime by up to 0.3 °C. This finding is similar to the results of[6] on MHS in Nanjing, where urban irrigation increased daytime HI (0.5 °C) and reduced nighttime HI (0.6 °C). From the SI index (Fig. 1f), urban irrigation reduced MHS in the afternoon and evening with a maximum reduction of 1.7 °C, but urban irrigation increased MHS in the morning up to 0.4 °C, and urban irrigation reduced MHS in rural areas with a maximum reduction of 0.6 °C, especially in the afternoon and evening.

Effect of different irrigation times on MHS

To further investigate the effect of different irrigation times on MHS, we selected eight times for irrigation experiments, and the results of the SI index are used as an example for this analysis. From irrigation at UTC 00:00 (Fig. 2a), irrigation reduced MHS in urban and surrounding regions, but it increased MHS in the western mountainous areas of Beijing. From irrigation at UTC 02:00 (Fig. 2b), irrigation increased MHS in urban and rural areas; at this time, that is, 10:00 local time, solar radiation was gradually stronger, and the land surface temperature was warming faster, although irrigation cooled down the temperature, the magnitude of its reduction was less than the rate of warming, followed by the enhancement of solar radiation, latent heat increase, and the relative humidity caused by irrigation also increased, so at this time irrigation increased MHS in urban and rural areas. From irrigation at UTC 04:00 (Fig. 2c), irrigation had a cooling effect on urban and rural areas, but the extent and magnitude of urban cooling was smaller than at UTC 00:00. From irrigation at UTC 11:00 (Fig. 2d), irrigation had a cooling effect on MHS in urban and rural areas, but the extent and magnitude of urban cooling was smaller than that at UTC 00:00 and 04:00, probably related to the fact that solar radiation slowly became 0 at this time, surface thermal radiation was enhanced, and the cooling caused by irrigation was smaller. From irrigation at UTC 13:00 and 15:00 (Fig. 2e, f), irrigation reduced MHS in urban and rural areas and was higher in magnitude than at other times. From irrigation at UTC 20:00 (Fig. 2g), irrigation reduced MHS in urban areas but increased it in rural areas, especially in the northeast of Beijing. From irrigation at UTC 22:00 (Fig. 2h), irrigation reduced MHS in urban areas but increased MHS in rural areas. Therefore, it can be seen that MHS in urban and rural areas responded differently to irrigation at different times, with irrigation at UTC 13:00 and 15:00 being more effective for MHS mitigation in Beijing.

To further quantify the effect of irrigation on MHS in urban areas under different irrigation times, we analyzed daily trends of irrigation on different MHS indices. It can be seen from the time series of AT index (Fig. 3a) that irrigation at different times of the day had different effects on different moments of the day, where irrigation at UTC 00:00 and 20:00 had a cooling effect on the daytime hours (UTC 00:00–04:00, it was morning for local time), while irrigation at other times increased MHS. Starting from UTC 08:00 to 23:00, except for 02:00 and 20:00, irrigation reduced MHS at other times. Meanwhile, we see from the box plot (Fig. 3b) that irrigation reduced MHS at all times except at UTC 02:00 and 20:00, with the largest MHS cooling caused by irrigation at UTC 00:00, which reduced up to 1.81 °C, and the largest MHS increase

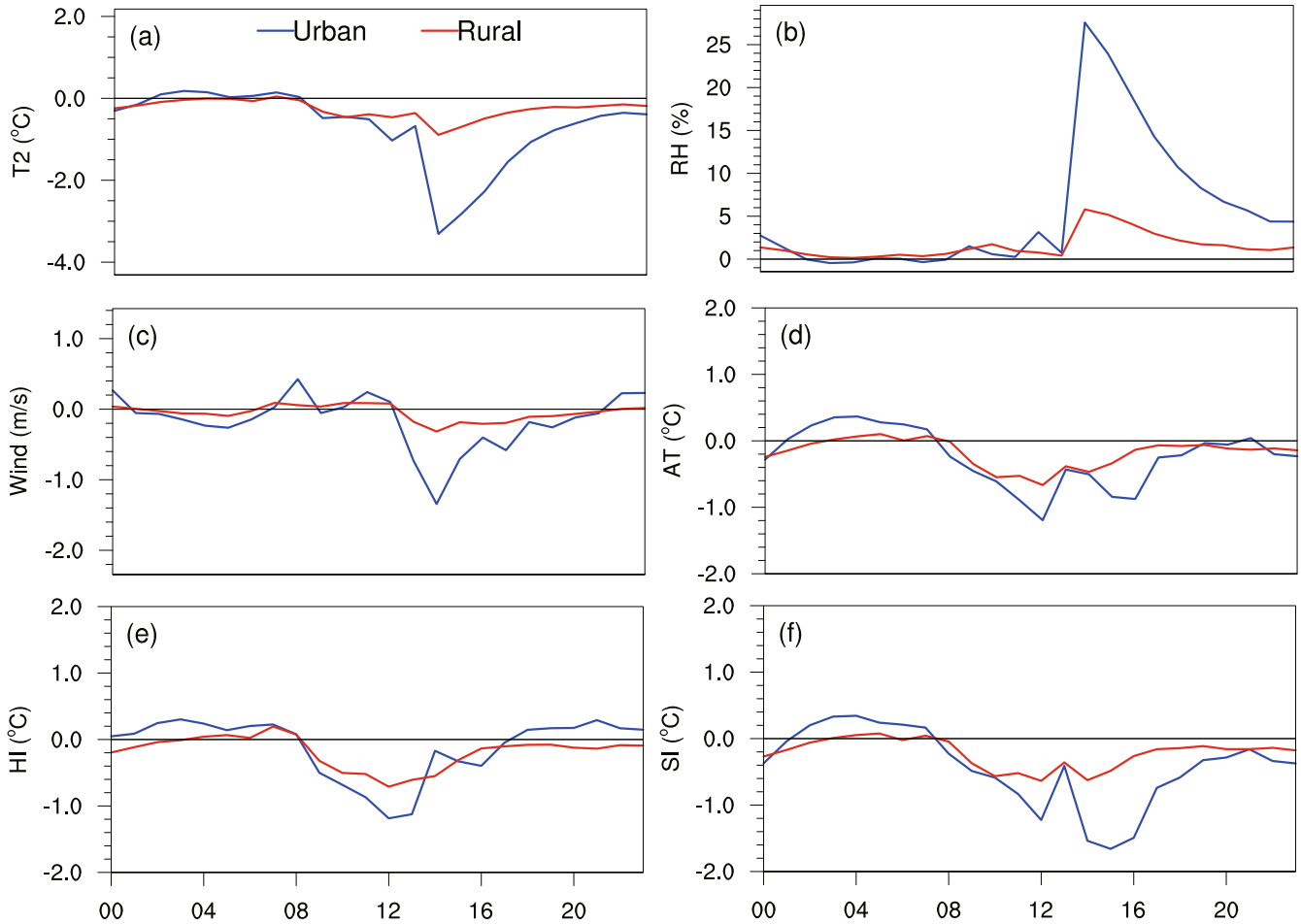

Fig. 1 Effect of urban irrigation on temperature, relative humidity, wind speed, and different MHS index in urban and rural. The results are the average from August 2nd to August 8th for the same hours every day; **a** temperature; **b** relative humidity; **c** wind speed; **d** AT; **e** HI; **f** SI, where the blue line is urban and the red line is rural; *x*-axis is UTC).

caused by irrigation was at UTC 02:00, which increased up to 1.35 °C. The average cooling effect of irrigation at UTC 13:00 and 15:00 was the best, with a reduction of 0.23 °C and 0.25 °C, respectively, followed by UTC 00:00 and 04:00. The time series of HI index showed (Fig. 3c) that irrigation at different times had different effects on MHS at different moments of the day, where irrigation at UTC 00:00, 15:00 and 20:00 had a cooling effect on the daytime hours, while irrigation at several other times increased MHS in urban areas. From UTC 08:00 to 16:00 each day, irrigation decreased MHS at other times except for UTC 02:00, 11:00 and 20:00 irrigation. From UTC 16:00–23:00 each day, UTC 13:00, 15:00 and 20:00 irrigation increased moist heat, while several other times reduced it. Meanwhile, we see from the box plot (Fig. 3d) that irrigation reduced MHS at all times except at UTC 02:00, 11:00, and 20:00, where irrigation at UTC 00:00 caused the largest cooling up to 1.22 °C, and irrigation at UTC 20:00 caused the largest increase up to 1.65 °C. The average cooling effect of irrigation at UTC 00:00 was optimal, followed by UTC 04:00 and 13:00. It can be seen from the SI index time series (Fig. 3e) that irrigation at different times of the day had different effects on MHS at different moments, where irrigation at UTC 00:00, 15:00, 20:00, and 22:00 had a cooling effect on the daytime hours, while irrigation at other times increased MHS in urban areas. From UTC 08:00–16:00 each day, irrigation reduced MHS in urban areas at several other times, except for 02:00 and 20:00. From UTC 16:00 to 23:00 each day, UTC 13:00, 15:00, and 22:00 had a greater cooling effect on MHS, and several other hours had a smaller effect on MHS. Meanwhile, we see from the box plot (Fig. 3f) that irrigation reduced MHS at all times except at UTC 02:00, 11:00, and 20:00, where irrigation at UTC 00:00 and 11:00 caused the greatest cooling with a maximum reduction of 2.65 °C and 2.61 °C, and irrigation at UTC 02:00 and 20:00 caused the greatest increase with a maximum increase of 1.28 °C and 1.16 °C. The average cooling effect of irrigation was optimal at UTC 13:00 and 15:00, with 0.42 °C and 0.41 °C, followed by UTC 00:00 and 11:00. In general, irrigation at UTC 02:00 and 20:00 increased MHS, while irrigation at other times reduced MHS in urban areas, with the best cooling effect of irrigation at these times for night, especially irrigation at UTC 00:00 and 13:00. The effects of irrigation on MHS in rural areas under different irrigation times can be found in Supplementary Fig. 6 in Supplementary Information).

DISCUSSION

This study revealed the cooling effect of urban irrigation on MHS in urban and rural areas, as well as the effect of different irrigation times on MHS in Beijing through sensitivity experiments, which can provide a basis for mitigating MHS under urban heat islands and future urban planning in Beijing. The findings of this study are consistent with other related studies that urban irrigation can reduce the temperature in Phoenix by up to 3 °C and contribute to the thermal comfort of urban residents[30]; 90% of the water supply in Beijing is used for urban irrigation, and 10% for road sprinkling, which can reduce summer temperatures in the Beijing area by

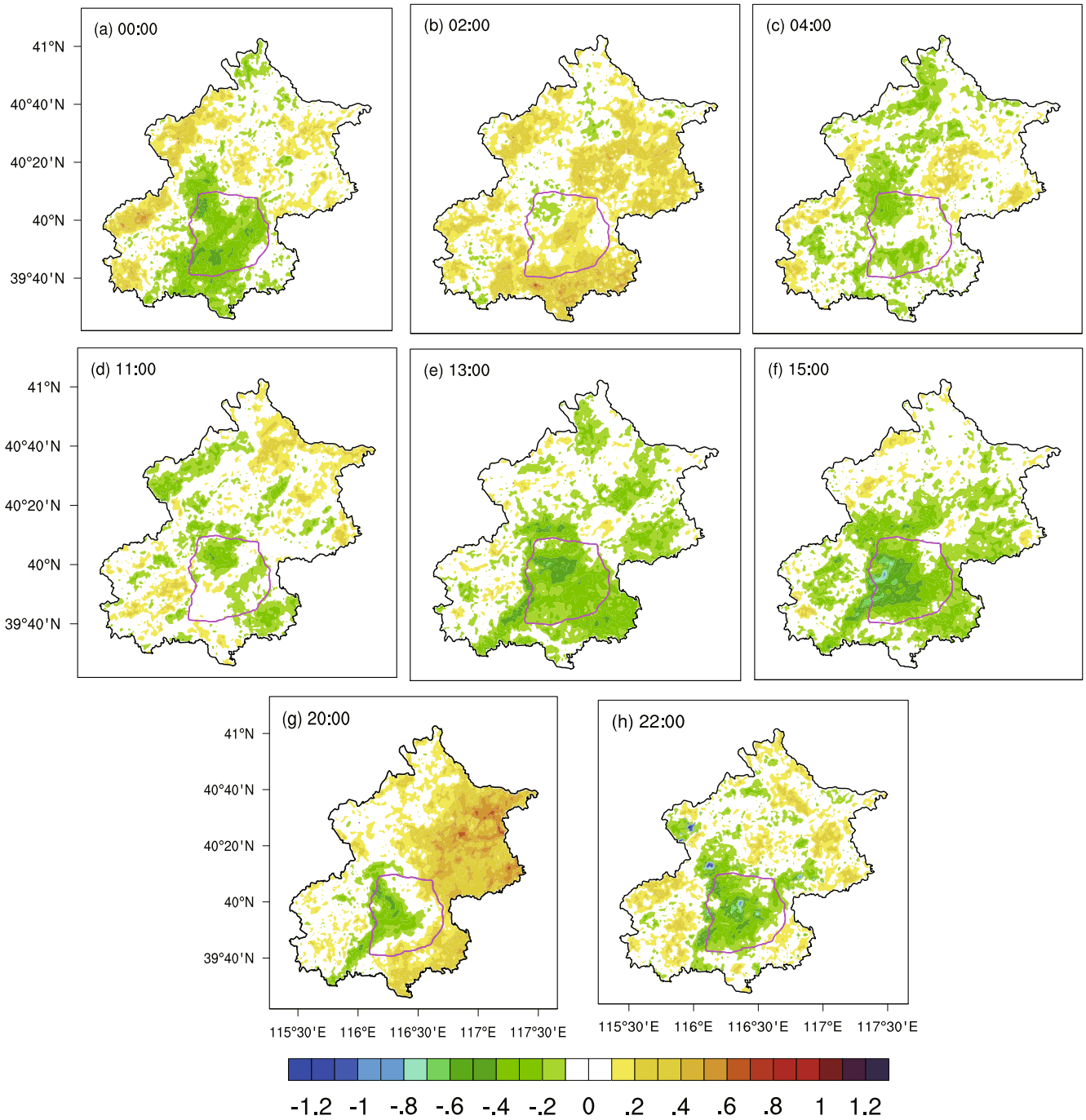

Fig. 2 Effect of different irrigation times on MHS in Beijing. a UTC 00:00; **b** UTC 02:00; **c** UTC 04:00; **d** UTC 11:00; **e** UTC 13:00; **f** UTC 15:00; **g** UTC 20:00; **h** UTC 22:00.

1.9 °C[16], and that urban irrigation can reduce MHS in Nanjing, especially for the MHS at night[6].

In addition to the effect of irrigation on MHS, there are also corresponding attempts to reduce urban MHS by increasing the surface albedo, which increases solar radiation absorbed by the city and decreases the surface temperature and air temperature[31]. For example, green roofs can reduce surface temperatures and sensible heat fluxes and improve building energy efficiency[32], and human heat stress in urban environments can also be countered by deploying solar panels on rooftops or by utilizing cool roofs with high albedo[33].

This study only analyzed the impact of urban irrigation on the hygrothermal regime in Beijing, while China has more mega-city clusters, such as the Yangtze River Delta, Pearl River Delta, and Chengdu-Chongqing urban clusters, which are located in different climate zones. The effect of irrigation on MHS may depend heavily on climate types with irrigation-induced increasing relative humidity, which may have different effects on wet heat in humid and arid areas[34]. In the context of global warming, what are the mechanisms of irrigation's hygrothermal impacts on other urban agglomerations in China under different climate types? This is one of our next tasks.

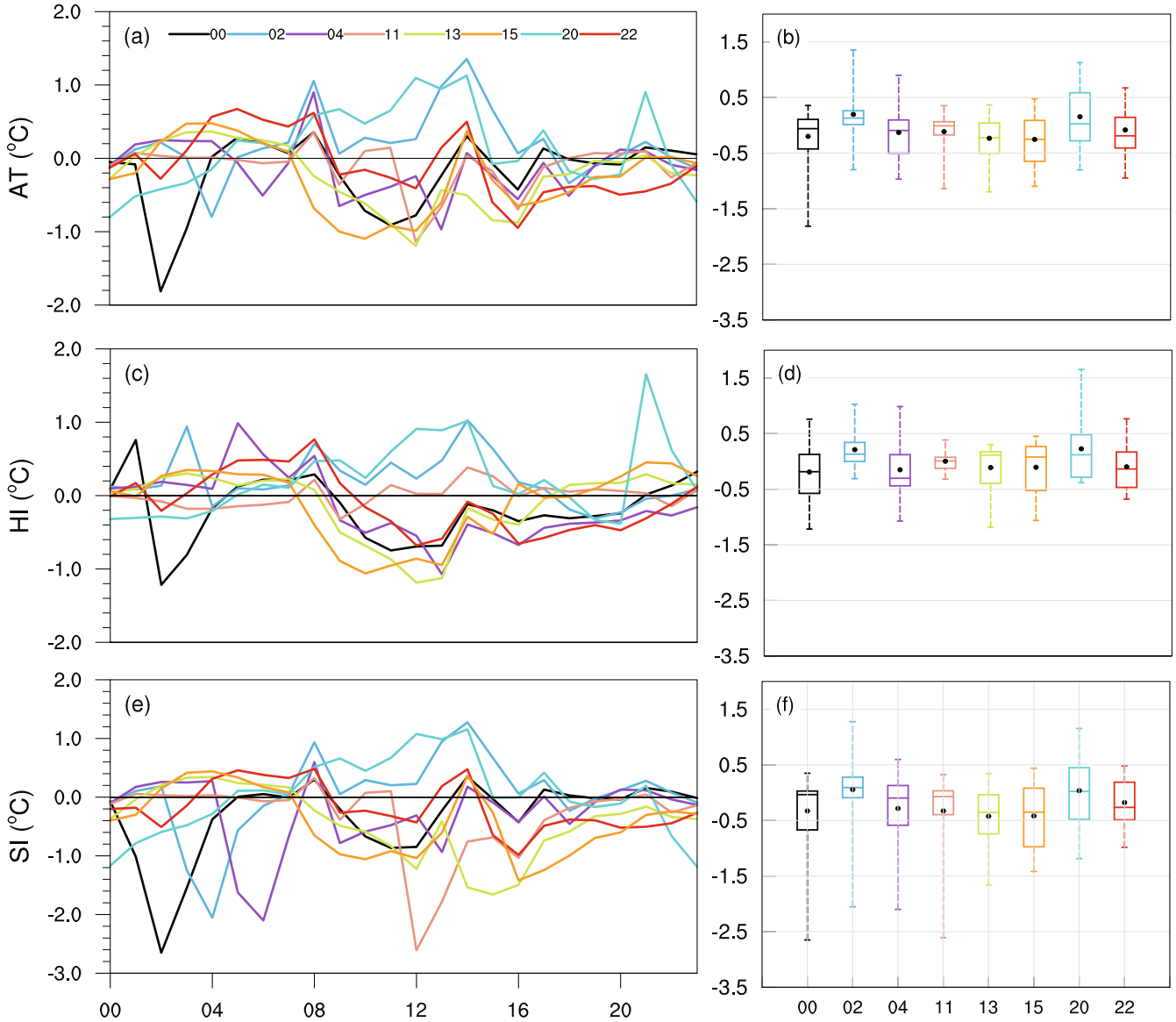

Fig. 3 Effect of different irrigation times on MHS in urban areas. The results are the average from August 2 to August 8 for the same hours every day; **a**, **b** AT; **c**, **d** HI: **e**, **f** SI; x-axis is UTC.

METHODS

We used the WRF-SLUCM to analyze the effects of irrigation on MHS. The introduction of the WRF-SLUCM and the parameterization scheme configuration of the model can be found in Section 1.1 of Supplementary Information. The introduction of initial and boundary conditions data (FNL, CRA, CRA_CLDAS) that drive the WRF-SLUCM model can be found in section 1.2 of Supplementary Information. The introduction of site observation data that was used to evaluate temperature, relative humidity, and wind speed simulated by the WRF-SLUCM can be found in Section 1.3 of Supplementary Information. Further, the calculation formulas for the bias and root mean square error (RMSE) can be found in Section 1.4 of Supplementary Information.

Experimental design

We chose July 12 to July 25, 2022, and August 2–August 8, 2022, for the analysis of MHS. Considering the Beijing Meteorological Station issued continuous yellow warnings for high temperatures, and the maximum temperature in most areas of Beijing reached about 35 °C with high relative humidity from August 2 to August 8, 2022, we analyzed this individual case from August in detail. The analysis of the July case can be found in Section 3 of the Supplementary Information. We used three nested layers for the simulation analysis of humid heat events in Beijing (9 km, 3 km, and 1 km, respectively) (Fig. 4).

First, we verified the simulation effect of WRF that turns off the irrigation on temperature, relative humidity, and wind speed in Beijing. We used FNL, CRA, and CRA_CLDAS to simulate temperature, relative humidity, and wind speed at 1 km/1 h in the Beijing area, evaluated them using station observations, and calculated the bias, root mean square error (RMSE) of the temperature, relative humidity, and wind speed simulated by WRF under FNL, CRA, and CRA_CLDAS.

Secondly, we turned urban irrigation on and off for the WRF-SLUCM to analyze its effect on land surface variables and MHS in urban and rural areas, respectively. For the configuration of urban irrigation parameters in Beijing, according to the quality standard for urban road cleaning issued by the Beijing Municipal Administration of Quality and Technology Supervision (NO: DB11/T 353-2006), urban irrigation is activated only in summer

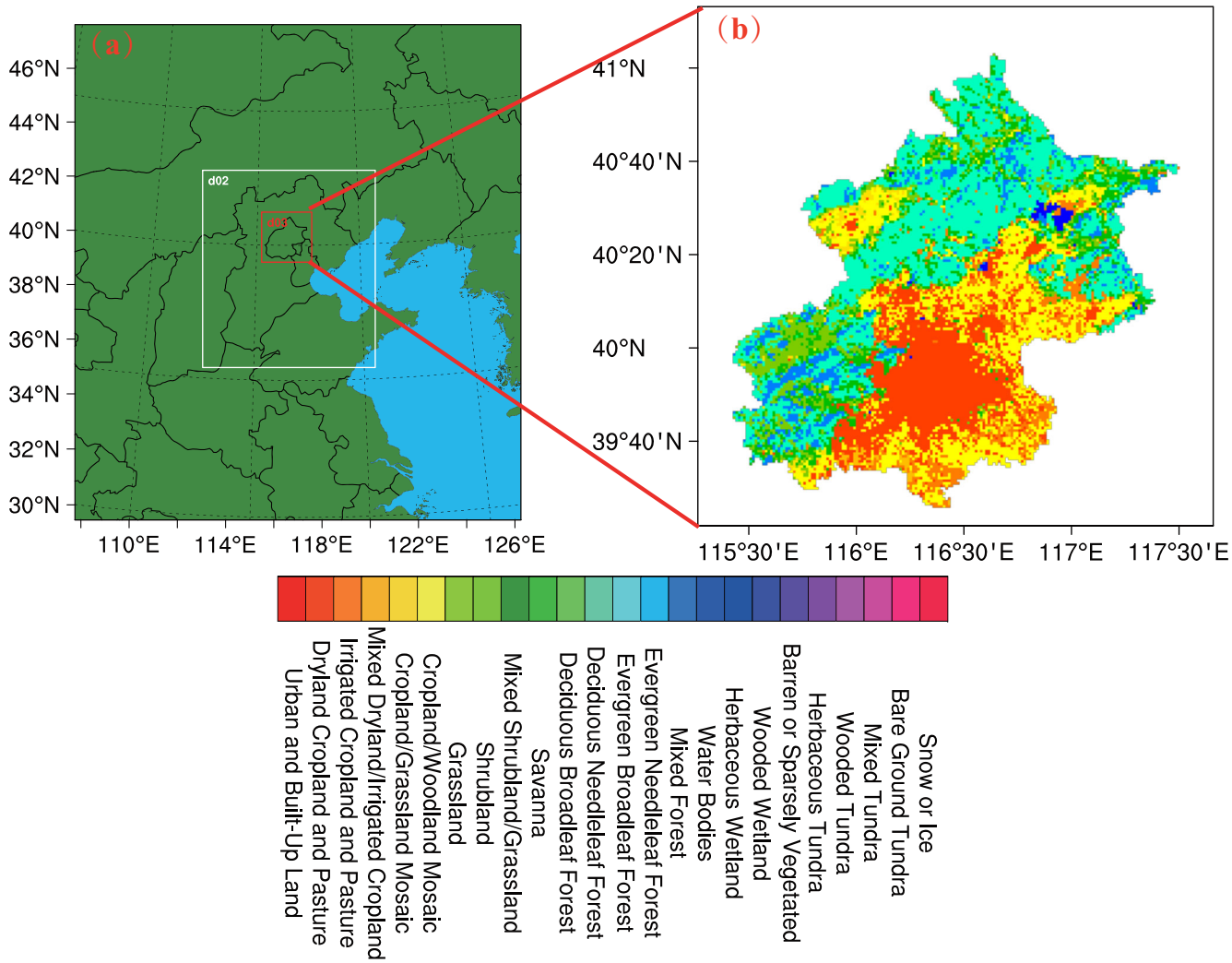

Fig. 4 Study area and surface cover types of Beijing. a The three nested layers for the simulation of WRF-SLUCM; **b** the land cover classification of Beijing.

nights, and we chose 13 UTC for a duration of 2 h. Considering that the irrigation method in Beijing is mainly traditional sprinkler irrigation, the " sprinkler scheme" was chosen[16].

To further investigate the effect of urban irrigation on MHS at different times, eight sets of comparative experiments were designed to analyze the effect of irrigation on MHS at different times by setting the irrigation time to 00:00, 02:00, 04:00,11:00, 13:00,15:00, 20:00, and 22:00 UTC, respectively.

MHS index

In hot summer environments, the human body actually feels much warmer than the air temperature shows, mainly because the humidity in the environment reduces the body's ability to cool itself, hence the inclusion of relative humidity in the study of heat stress; however, many studies have shown that there is no uniform indicator of MHS for different environmental conditions and climatic background conditions[35–37]. In order to reduce the uncertainty introduced by the MHS in this study, three widely—used indexes were used here.

AT represents the thermal sensation of a person walking outdoors in the shade, and its calculation takes into account air temperature and wind speed[38]. AT can be computed as:

$$\mathrm{AT} = T + 0.33 \times P - 0.7 \times V - 4.0 \quad (1)$$

$$P = \mathrm{RH}/100 \times 6.105 \times e^{(17.27 \times T/(273.7+T))} \quad (2)$$

The HI has been widely used for the evaluation of indoor and outdoor thermal conditions and human comfort[39]. It can be computed as:

$$\mathrm{HI} = T + 0.5555 \times (P - 10) \quad (3)$$

The SI is a general formula for apparent temperature, an integrated measure of overall climatic variables affecting human comfort and behavior[36]. It can be calculated as:

$$\mathrm{SI} = 1.07 \times T + 0.2 \times P - 0.65 \times V - 2.7 \quad (4)$$

where T denotes the air temperature, RH denotes the relative humidity, P is vapor pressure, and V denotes the wind speed.

DATA AVAILABILITY

The in-situ observations, the CRA, and the CLDAS soil moisture datasets are sourced from http://data.cma.cn. The FNL datasets are obtained from

http://rda.ucar.edu/datasets/ds083.2/. The soil texture data for WRF simulation are sourced from http://globalchange.bnu.edu.cn/research/soilw. The land cover data for WRF simulation are sourced from https://www.esa-landcover-cci.org/. The other datasets used in this current study are accessible from the corresponding author on reasonable request.

CODE AVAILABILITY

The WRF 4.3 source code is from https://github.com/wrf-model. The other source code used in this current study is accessible from the corresponding author on reasonable request.

Received: 16 October 2023; Accepted: 24 January 2024;
Published online: 05 February 2024

REFERENCES

1. Pörtner, H. O. et al. IPCC 2022: Technical Summary, Working Group II Impacts, Adaptation and Vulnerability. 3–33 (2023).
2. Wang, G., Zhang, Q., Luo, M., Singh, V. P. & Xu, C. Y. Fractional contribution of global warming and regional urbanization to intensifying regional heatwaves across Eurasia. *Clim. Dyn.* **59**, 1521–1537 (2022).
3. You, Q. et al. A comparison of heat wave climatologies and trends in China based on multiple definitions. *Clim. Dyn.* **48**, 3975–3989 (2017).
4. Xu, H. et al. Long-term spatiotemporal patterns and evolution of regional heat islands in the Beijing–Tianjin–Hebei urban agglomeration. *Remote Sens.* **14**, 2478 (2022).
5. Zhang, Q., Wu, Z., Yu, H., Zhu, X. & Shen, Z. Variable urbanization warming effects across metropolitans of China and relevant driving factors. *Remote Sens.* **12**, 1500 (2020).
6. Wang, X. et al. Effectiveness of urban hydrological processes in mitigating urban heat island and human thermal stress during a heat wave event in Nanjing, China. *J. Geophys. Res.* **125**, e2020JD033275 (2020).
7. Jeong, S., Millstein, D. & Levinson, R. Modeling potential air temperature reductions yielded by cool roofs and urban irrigation in the Kansas City Metropolitan Area. *Urban Clim.* **37**, 100833 (2021).
8. Yuan, Y. et al. Natural-anthropogenic environment interactively causes the surface urban heat island intensity variations in global climate zones. *Environ. Int.* **170**, 107574 (2022).
9. Kumar, R. & Mishra, V. Decline in surface urban heat island intensity in India during heatwaves. *Environ. Res. Commun.* **1**, 031001 (2019).
10. Gao, K., Santamouris, M. & Feng, J. On the cooling potential of irrigation to mitigate urban heat island. *Sci. Total Environ.* **740**, 139754 (2020).
11. Davis, R. E., Knappenberger, P. C., Michaels, P. J. & Novicoff, W. M. Changing heat-related mortality in the United States. *Environ. Health Persp.* **111**, 1712–1718 (2003).
12. Cai, W. et al. The 2021 China report of the Lancet Countdown on health and climate change: seizing the window of opportunity. *Lancet Public Health* **6**, e932–e947 (2021).
13. Russo, S. et al. Half a degree and rapid socioeconomic development matter for heatwave risk. *Nat. Commun.* **10**, 136 (2019).
14. Willett, K. M. & Sherwood, S. Exceedance of heat index thresholds for 15 regions under a warming climate using the wet-bulb globe temperature. *Int. J. Climatol.* **32**, 161–177 (2012).
15. Guo, Q., Zhou, X., Satoh, Y. & Oki, T. Irrigated cropland expansion exacerbates the urban moist heat stress in northern India. *Environ. Res. Lett.* **17**, 054013 (2022).
16. Liu, B. et al. Optimal water use strategies for mitigating high urban temperatures. *Hydrol. Earth Syst. Sci.* **25**, 387–400 (2021).
17. Meng, Q. et al. Characterizing spatial and temporal trends of surface urban heat island effect in an urban main built-up area: a 12-year case study in Beijing, China. *Remote Sens. Environ.* **204**, 826–837 (2018).
18. Liu, X. et al. Spatiotemporal patterns of summer urban heat island in Beijing, China using an improved land surface temperature. *J. Clean. Prod.* **257**, 120519 (2020).
19. Liang, T. et al. Simulation of the influence of a fine-scale urban underlying surface on the urban heat island effect in Beijing. *Atmos. Res.* **262**, 105786 (2021).
20. Dai, Z., Guldmann, J. M. & Hu, Y. Spatial regression models of park and land-use impacts on the urban heat island in central Beijing. *Sci. Total Environ.* **626**, 1136–1147 (2018).
21. Liu, R. et al. The impacts of urban anthropogenic heat and surface albedo change on boundary layer meteorology and air pollutants in the Beijing-Tianjin-Hebei region. *Urban Clim.* **47**, 101358 (2023).
22. Wang, Y. et al. Appraising regional anthropogenic heat flux using high spatial resolution NTL and POI data: a case study in the Beijing-Tianjin-Hebei region, China. *Environ. Pollut.* **292**, 118359 (2022).
23. Yang, P., Ren, G. & Hou, W. Impact of daytime precipitation duration on urban heat island intensity over Beijing city. *Urban Clim.* **28**, 100463 (2019).
24. Miao, Y., Che, H., Liu, S. & Zhang, X. Heat stress in Beijing and its relationship with boundary layer structure and air pollution. *Atmos. Environ.* **282**, 119159 (2022).
25. Yang, G. et al. PM2.5 influence on urban heat island (UHI) effect in beijing and the possible mechanisms. *J. Geophys. Res.* **126**, e2021JD035227 (2021).
26. Banta, R. & Gannon, P. Influence of soil moisture on simulations of katabatic flow. *Theor. Appl. Climatol.* **52**, 85–94 (1995).
27. Santanello, J. A. Jr, Lawston, P., Kumar, S. & Dennis, E. Understanding the impacts of soil moisture initial conditions on NWP in the context of land–atmosphere coupling. *J. Hydrometeorol.* **20**, 793–819 (2019).
28. Mueller, N. D. et al. Cooling of US Midwest summer temperature extremes from cropland intensification. *Nat. Clim. Change* **6**, 317–322 (2016).
29. Puma, M. & Cook, B. Effects of irrigation on global climate during the 20th century. *J. Geophys. Res.* **115**, D16 (2010).
30. Yang, J. & Wang, Z. H. Optimizing urban irrigation schemes for the trade-off between energy and water consumption. *Energy Build.* **107**, 335–344 (2015).
31. Salamanca, F., Georgescu, M., Mahalov, A., Moustaoui, M. & Martilli, A. Citywide impacts of cool roof and rooftop solar photovoltaic deployment on near-surface air temperature and cooling energy demand. *Bound-Lay. Meteorol.* **161**, 203–221 (2016).
32. Yang, J. et al. Enhancing hydrologic modelling in the coupled weather research and forecasting–urban modelling system. *Bound-Lay. Meteorol.* **155**, 87–109 (2015).
33. Ma, S. et al. Evaluating the effectiveness of mitigation options on heat stress for Sydney, Australia. *J. Appl. Meteorol. Clim.* **57**, 209–220 (2018).
34. Cheung, P. K., Livesley, S. J. & Nice, K. A. Estimating the cooling potential of irrigating green spaces in 100 global cities with arid, temperate or continental climates. *Sustain Cities Soc.* **71**, 102974 (2021).
35. Montero, J. C., Miron, I. J., Criado, J. J., Linares, C. & Díaz, J. Difficulties of defining the term,"heat wave", in public health. *Int. J. Environ. Health Res.* **23**, 377–379 (2013).
36. Wang, X. et al. Assessing the impact of urban hydrological processes on the summertime urban climate in Nanjing using the WRF model. *J. Geophys. Res.* **124**, 12683–12707 (2019).
37. Buzan, J. R., Oleson, K. & Huber, M. Implementation and comparison of a suite of heat stress metrics within the Community Land Model version 4.5. *Geosci. Model Dev.* **8**, 151–170 (2015).
38. Steadman, R. G. A universal scale of apparent temperature. *J. Appl. Meteorol. Clim.* **23**, 1674–1687 (1984).
39. Masterton, J. M., & Richardson, F. A. Humidex: a method of quantifying human discomfort due to excessive heat and humidity. *Environment Canada, Atmospheric Environment*, 35–36 (Academic, 1979).

ACKNOWLEDGEMENTS

This research has been supported by the China National Key R&D Program (Grant No. 2019YFA0606900), Open Foundation of the Key Laboratory of Coupling Process and Effect of Natural Resources Elements (No. 2022KFKTC003), Advance research on civil space technology during China's 14th Five-Year Plan (D040405), the National Science Foundation of China (Grant No. 41771536, No. 42161054, No.42375040), the satellite application advance plan of Feng-Yun (Grant No. FY-APP-2022.0608) and the National Meteorological Information Center balance project (Grant No. NMICJY202104 and No. NMICJY202207).

AUTHOR CONTRIBUTIONS

S.S. and Z.Q. conceived the study and designed the experimental approach; S.S., S.C.X., Z.T., C.D.H., and W.G. performed the analyses and generated the results. S.S., G.J.X., W.J.M., and W.W.H. plotted and edited the figures in the paper. All authors contributed to the formulation of the study, analyses, and revisions of the paper.

COMPETING INTERESTS

The authors declare no competing interests.

ADDITIONAL INFORMATION

Supplementary information The online version contains supplementary material available at https://doi.org/10.1038/s41612-024-00585-6.

Correspondence and requests for materials should be addressed to Qiang Zhang.

Reprints and permission information is available at http://www.nature.com/reprints

Publisher's note Springer Nature remains neutral with regard to jurisdictional claims in published maps and institutional affiliations.